

# Functional Metamaterial Devices Enabled by Microsystems

X. Zhang<sup>1</sup>, and X. Zhao<sup>1,2</sup>

<sup>1</sup>Department of Mechanical Engineering and Photonics Center, Boston, MA, USA. email: xinz@bu.edu

<sup>2</sup>Department of Radiology, Boston, MA, USA

**Abstract**—Metamaterials represent a class of artificially engineered materials, which exhibit unprecedented properties enabled by their constituent subwavelength unit cells. The effective properties of metamaterials may be dynamically controlled by driving unit cells via different approaches, including photo-doping, electrical gating, or mechanical actuation. With such dynamical tuning mechanisms, the propagation modality of electromagnetic waves may be modulated to achieve functional devices for modulation, beam steering, focusing, and polarization control, among others. In addition, the perfect absorption and near field effect enabled by metamaterials may be used in electromagnetic detectors across the frequency spectrum. Microsystem technology provides a platform to achieve functional metamaterial devices by covering all requisite processes, including fabrication, packaging, and system integration. We report our progress in constructing functional devices by integrating metamaterials with microsystems technology and discuss remaining challenges and the future direction of metamaterial devices.

## I. INTRODUCTION

Electromagnetic (EM) metamaterials are an important category of artificial materials consisting of subwavelength unit cells. By designing the geometry of the unit cells, the effective properties, such as effective permittivity and permeability, of the metamaterials may be engineered, which, in turn, controls the scattering and/or absorption of electromagnetic (EM) waves. Beginning with the experimental demonstration of negative index materials [1], metamaterials have enabled many unique applications and capabilities, such as invisibility cloaking [2], perfect absorption [3], and superlensing [4]. Following that, the 2D metamaterials, i.e., metasurfaces, featuring a single layer surface consisting of in plane subwavelength unit cells have been developed to manipulate the EM wave. Metasurface-based optical components, including metalenses [5], metamirrors [6], metagratings [7], phase plates for orbital angular momentum (OAM) [8], have been developed to focus, steer, or spin EM waves. Recent advances in condensed matter theory have inspired novel metamaterial properties, such as topologically protected edge states [9,10], parity-time symmetry [11] and exceptional points [12], giving rise to more versatile control over these man-made material properties. The rapid development of the understanding of the relevant physics and science in designing metamaterials has allowed for the rapid translation of metamaterials from fundamental research to practical applications to overcome current limitations in our physical

systems. For example, in short order, passive infrared metamaterials has been developed to radiatively cool buildings for high-efficiency thermal management, addressing an unmet, practical societal need [13].

In order to enhance metamaterial functionalities, a hot topic in current research in metamaterials is the construction of reconfigurable, tunable, nonlinear, and self-adaptive metamaterials towards metamaterial devices, or namely metadevices [14]. Leveraging metamaterials, dynamical tunability would enable real-time modulation of the EM response, thereby achieving high-efficiency manipulation of EM waves in a compact geometry. Microsystems technology, or microelectromechanical systems (MEMS), provides a platform to construct metamaterial devices. The development of metamaterials is facilitated by advances in micro-/nano-fabrication processes, which are an essential part of microsystems technology. In addition, MEMS provides numerous tools to reconfigure metamaterials or enable novel metamaterial functionalities [15,16].

The combination of microsystems and metamaterials was initially implemented in thermo-mechanically reconfigurable terahertz metamaterials [17], which demonstrated the feasibility of tuning metamaterial responses via mechanical displacement. Subsequently, research related to microsystems-enabled metamaterials thrived, yielding various reconfigurable and tunable metamaterials in the spectral range from the microwave to optical regimes [18]. Herein, we report our progress related to functional metamaterial devices enabled by microsystems technology. A typical integration scheme between metamaterials and microsystems will be introduced and the general outlook related to the ongoing development of microsystems-based metamaterial devices will be discussed.

## II. DYNAMIC METAMATERIALS DRIVEN BY MICROSYSTEMS

Microsystem technology covers the fabrication processes, system integration, and packaging of miniaturized, integrated transducers, including sensors and actuators [19]. Miniaturized actuators, such as electrostatic, thermo-mechanical, piezoelectric, and magnetic actuators, may be used to drive the mechanical displacement in the metamaterials in order to tune their effective properties [20]. As shown in Fig. 1, the MEMS actuators may reconfigure the geometry of split ring resonators, which are a typical metamaterial structure, in order to modify the resonance frequency of the metamaterials, thereby, change their effective permittivity ( $\epsilon$ ). Simulation results (Figs. 1c and

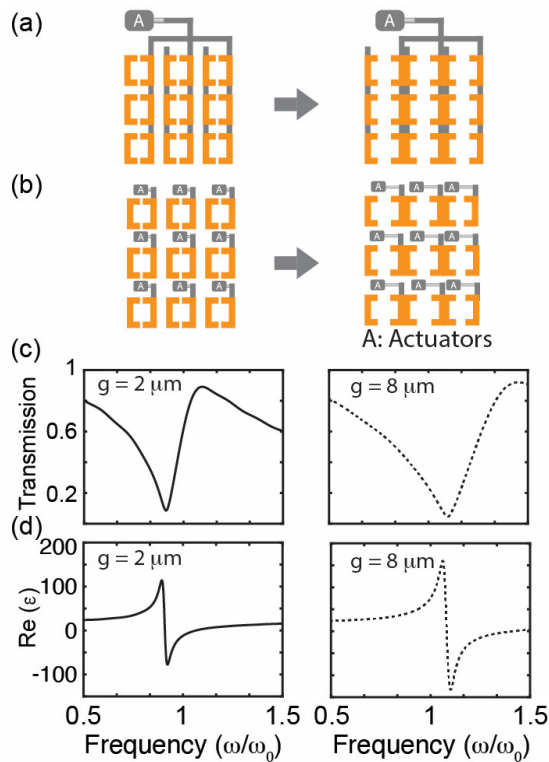


Figure 1. Illustration of dynamic metamaterials driven by microsystems. (a) Schematic of homogeneously actuated metamaterials. (b) Schematic of individually actuated metamaterials. (c) Resonant transmission response for different gap sizes actuated by MEMS actuators. (d) Real part of Lorentz-like effective permittivity for different gap sizes.

1d) demonstrate the capability to tune the material properties across a large range, which can be translated to the manipulation of EM waves. MEMS actuators may be used to control either the entire array of the metamaterial for homogeneous modulation, or individual unit cells for local modulation. Homogeneous actuation may control amplitude [21], phase [22], polarization [23], and chirality [24]. Individually controllable unit cell may achieve additional functionalities, such as beam focusing, steering [25-28], and orbital angular momentum manipulation [29]. The homogeneously reconfiguring scheme provides an easy-for-integration design while the individually reconfiguring scheme enables additional functionalities but increases the complexity related to system integration.

In addition to reconfiguring unit cell geometry, MEMS actuators enable the reconfiguration of the relative angle between the incident wave and the metamaterial [17], as well as the coupling between adjacent unit cells [30,31], both of which yield control of the metamaterial response. Ultimately, the rational integration of MEMS actuators and metamaterials provides various degrees of freedom by which to control the properties of metamaterials.

### III. METMATERIAL ENHANCED MICROSYSTEMS

Metamaterials enable strong absorption and near field confinement/enhancement effects [32,33]. The near-field enhancement effect may be applied, for example, to achieve

highly sensitive chemical/biological detection [33]. The field confinement effect may also induce photothermal and electrostatic forces for electromechanical readout sensors for low-energy radiation, including terahertz or mid-infrared [34]. Metamaterial perfect absorbers (MPAs), which absorb the incident radiation and convert the EM energy to heat, may be integrated with bi-material, thermo-mechanical transducers to achieve high-performance detection and imaging devices [35-37]. However, these types of devices require complicated processes involving thin-film deposition and releasing steps, increasing the complexity of the fabrication and decreasing the yield. We designed and developed long-wave, mid-infrared, uncooled focal plane arrays (FPA) with simplified fabrication processes to integrate metamaterial perfect absorbers with bi-material detectors.

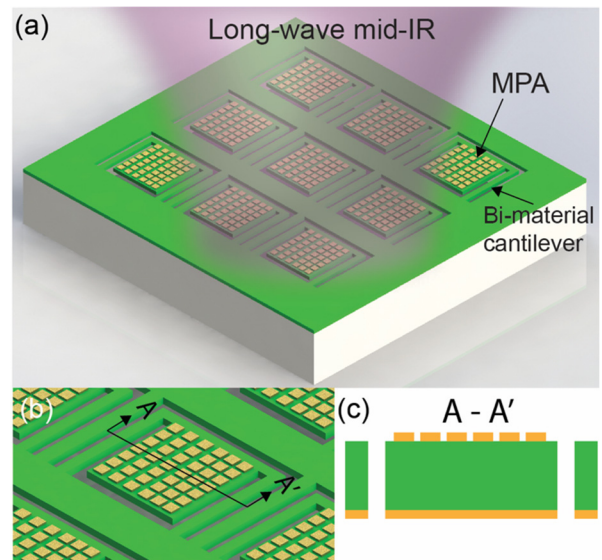


Figure 2. Schematic of the uncooled focal plane array (FPA) with integrated metamaterial perfect absorber (MPA). (a) Overall structure of the FPA, in which each pixel consists of an MPA and a bi-material cantilever. (b) Close-up view of a single pixel in the FPA. (c) Cross-sectional view of each detection pixel.

The designed FPA consists of an array of bi-material cantilever-supported MPA patches, which include gold squares patterned on a  $\text{SiN}_x$  spacer backed with a gold ground plane, as shown in Fig. 2a. In an FPA pixel (Fig. 2b), the MPA absorbs the incident infrared radiation and converts it to heat, deflecting the bi-material cantilever. The metal thin film serves as the ground plane of the MPA and metal layer for the bi-material thermal detector. The metamaterial is an array of periodic square patches patterned on the silicon nitride spacers, which is backed by the gold ground plane, forming a metal/insulator/metal (MIM) perfect absorber. Furthermore, the large coefficient of thermal expansion (CTE) mismatch between gold and silicon nitride enables the detection of temperature variations due to infrared radiation absorption. An optical readout platform, which sheds a light on the backside of the FPA, is used to detect the reflected light from the ground plane. By mapping the deflection of each pixel, an infrared image of an object can be captured by the detection system.

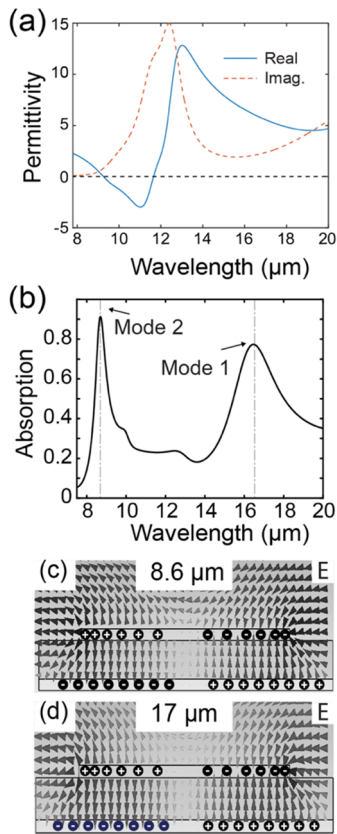


Figure 3. Design of the mid-IR metamaterial perfect absorber (MPA). (a) Permittivity of the SiN<sub>x</sub> dielectric spacer retrieved from the experimental characterization of the SiN<sub>x</sub> thin films. (b) Simulated absorption spectrum of a metamaterial perfect absorber with a sidewidth of 2.9 μm and a periodicity of 3.9 μm. (c) and (d) are the electric field distribution in the vicinity of the MPA at the shorter and longer wavelength modes, respectively.

In order to design the MPA, we first characterized the permittivity of the silicon nitride film (Fig. 2a) and utilized finite difference time domain (FDTD) numerical simulations to optimize the geometry of the metamaterial unit cells. We measured the reflection spectrum of a free-standing silicon nitride thin film using Fourier transform infrared (FTIR) spectroscopy. The Maxwell-Helmholtz-Drude dispersion model was employed to fit the reflection response [38] and the dispersion was obtained as shown in Fig. 2a. We employed the FDTD simulation to maximize the absorption in the vicinity of 8.6 μm using CST Microwave Studio. In the simulations, the periodic boundary condition was employed. Gold was modeled with the Drude response and the extracted silicon nitride permittivity was employed. The optimized side-width, periodicity, and silicon nitride thickness of the MPA are 2.9 μm, 3.9 μm, and 400 nm, respectively, as shown in Fig. 2b. There are two response modes in the absorption spectrum due to the dispersion of silicon nitride, corresponding to the dipolar resonant modes in the metamaterial unit cell, as shown in Figs. 3c and 3d.

To fabricate the FPA, low stress SiN<sub>x</sub> thin films were first deposited on a silicon wafer using low pressure chemical vapor deposition (LPCVD) (Fig. 4a). The metamaterial layer was then

patterned using a lift-off process (Fig. 4b), followed by SiN<sub>x</sub> etching to define the cantilevers (Fig. 4c). The backside of the SiN<sub>x</sub> was defined (Fig. 4d) by substrate through-etching to release the structure (Fig. 4e). The final step was to coat the backside with the gold ground plane (Fig. 4f). In comparison with [36], the fabrication process is simplified by the improved integration scheme, in which the back side gold layer serves as the ground plane for the MPA and active layer for the bi-material beams. The fabricated MPA exhibited perfect absorption at the designated wavelength, as shown in Fig. 3b. The temperature sensitivity of the bi-material cantilever is 0.13 μm/K. We placed the FPA in an optical readout platform consisting of an IR lens, a light-emitting diode (LED), and a CMOS camera to derive the image. Using this approach enables the capture of infrared images in the atmosphere and under uncooled conditions.

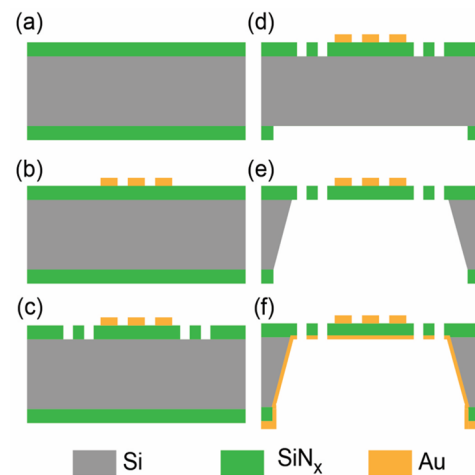


Figure 4. Fabrication processes of the uncooled focal plane array. (a) LPCVD growth of low stress SiN<sub>x</sub> thin films. (b) Patterning metamaterial layer. (c) Reactive ion etching of SiN<sub>x</sub> thin film. (d) Etching the backside SiN<sub>x</sub> layer. (e) Wet etching of SiN<sub>x</sub> substrate. (f) Deposition of the gold ground plane.

The fabrication process and developed device demonstrate the integration between metamaterials and microsystems for enhanced sensing applications.

#### IV. OUTLOOK

Future opportunities in metamaterials research include the development of metamaterials with multiple functionalities and self-adaptive responses enabled through the integration with microsystems. For example, a metamaterial device may manipulate EM wave propagation, while simultaneously sensing the incident wave. In this fashion, the beam manipulation may be altered based on the incident wave. This would enable metamaterials with self-adaptive, or smart, responses. Some early efforts in achieving self-adaptive metamaterials based on nonlinear response have led to smart metamaterials capable of manipulating the magnetic field for medical imaging and nonreciprocal devices [39,40]. By further optimizing the system integration schemes, advanced, smart metamaterials may be developed to blur the boundary between materials and devices, yielding high-performance, multifunctional devices.

## ACKNOWLEDGMENT

The authors acknowledge the National Science Foundation under Grant ECCS-1810252. We also gratefully acknowledge Northrop Grumman's support of this research project on metamaterial enhanced focal plan arrays.

## REFERENCES

- [1] R.A. Shelby, R. A., D.R. Smith, and S. Schultz, "Experimental verification of a negative index of refraction." *Science* vol. 292, pp. 77–79 (2001).
- [2] D. Schurig, J. J. Mock, B. J. Justice, S. A. Cummer, J. B. Pendry, A. F. Starr, and D. R. Smith, "Metamaterial electromagnetic cloak at microwave frequencies." *Science* vol. 314, pp. 977–980 (2006).
- [3] N. I. Landy, S. Sajuyigbe, J. J. Mock, D. R. Smith, and W. J. Padilla, "Perfect metamaterial absorber." *Phys. Rev. Lett.* vol. 100, 207402 (2008).
- [4] N. Fang, H. Lee, C. Sun, and X. Zhang, "Sub-diffraction-limited optical imaging with a silver superlens." *Science* vol. 308, pp. 534–537 (2005).
- [5] M. Khorasaninejad, W. T. Chen, R. C. Devlin, J. Oh, A. Y. Zhu, and F. Capasso, "Metalenses at visible wavelengths: Diffraction-limited focusing and subwavelength resolution imaging." *Science* vol. 352, pp. 1190–1194 (2016).
- [6] V. S. Asadchy, Y. Ra'di, J. Vehmas, and S. A. Tretyakov, "Functional metamirrors using bianisotropic elements." *Phys. Rev. Lett.* vol. 114, pp. 095503 (2015)
- [7] Y. Ra'di, D. L. Sounas, and A. Alu, "Metagratings: Beyond the limits of graded metasurfaces for wave front control." *Phys. Rev. Lett.* vol. 119, pp. 067404 (2017).
- [8] P. Genevet, N. Yu, F. Aieta, J. Lin, M. A. Kats, R. Blanchard, M. O. Scully, Z. Gaburro, and F. Capasso, "Ultra-thin plasmonic optical vortex plate based on phase discontinuities." *Appl. Phys. Lett.* vol. 100, pp. 013101 (2012).
- [9] X. Cheng, C. Jouvaud, X. Ni, H. Mousavi, A. Z. Genack, and A. B. Khanikaev. "Robust reconfigurable electromagnetic pathways within a photonic topological insulator." *Nat. Mater.* vol. 15, pp. 542–548 (2016).
- [10] Y. Yang, Y. Yamagami, X. Yu, P. Pitchappa, J. Webber, B. Zhang, M. Fujita, T. Nagatsuma, and R. Singh, "Terahertz topological photonics for on-chip communication." *Nat. Photon.* vol. 14, pp. 446–451 (2020).
- [11] L. Feng, Y.-L. Xu, W. S. Fegadolli, M.-H. Lu, J. E. B. Oliveira, V. R. Almeida, Y.-F. Chen, and A. Scherer, "Experimental demonstration of a unidirectional reflectionless parity-time metamaterial at optical frequencies." *Nat. Mater.* vol. 12, pp. 108–113 (2013).
- [12] M.-A. Miri, and A. Alu, "Exceptional points in optics and photonics." *Science* vol. 363, pp. eaar7709 (2019).
- [13] Y. Zhai, Y. Ma, S. N. David, R. Lou, G. Tan, R. Yang, and X. Yin, "Scalable-manufactured randomized glass-polymer hybrid metamaterial for daytime radiative cooling." *Science* vol. 355, pp. 1062–1066 (2017).
- [14] N. I. Zheludev, and Y. S. Kivshar, "From metamaterials to metadevices." *Nat. Mater.* vol. 11, pp. 917–924 (2012).
- [15] X. Zhao, G. Duan, A. Li, C. Chen, and X. Zhang, "Integrating microsystems with metamaterials towards metadevices." *Microsyst. Nanoeng.* vol. 5, pp. 5 (2019).
- [16] Z. Ren, Y. Chang, Y. Ma, K. Shih, B. Dong, and C. Lee, "Leveraging of MEMS technologies for optical metamaterials applications." *Adv. Opt. Mater.* vol. 8, pp.1900653 (2020).
- [17] H. Tao, A. C. Strikwerda, K. Fan, W. J. Padilla, X. Zhang, and R. D. Averitt, "Reconfigurable terahertz metamaterials." *Phys. Rev. Lett.* vol. 103, pp. 147401 (2009).
- [18] N. I. Zheludev, and E. Plum, "Reconfigurable nanomechanical photonic metamaterials." *Nat. Nanotechnol.* vol. 11, pp. 16–22 (2016).
- [19] C. Liu, *Foundations of MEMS*. (Pearson Education, 2011)
- [20] A. Q. Liu, W. M. Zhu, D. P. Tsai, and N. I. Zheludev, "Micromachined tunable metamaterials: A review." *J. Opt.* vol. 14, pp. 114009 (2012).
- [21] W. M. Zhu, A. Q. Liu, X. M. Zhang, D. P. Tsai, T. Bourouina, J. H. Teng, X. H. Zhang, H. C. Guo, H. Tanoto, T. Mei, G. Q. Lo, and D. L. Kwong, "Switchable magnetic metamaterials using micromachining processes." *Adv. Mater.* vol. 23, pp. 1792–1796 (2011).
- [22] X. Zhao, J. Zhang, K. Fan, G. Duan, J. Schalch, G. R. Keiser, R. D. Averitt, and X. Zhang, "Real-time tunable phase response and group delay in broadside coupled split-ring resonators." *Phys. Rev. B* vol. 99, pp. 245111 (2019).
- [23] X. Zhao, J. Schalch, J. Zhang, H. R. Seren, G. Duan, R. D. Averitt, and X. Zhang, "Electromechanically tunable metasurface transmission waveplate at terahertz frequencies." *Optica* vol. 5, pp. 303–310 (2018).
- [24] T. Kan, A. Isozaki, N. Kanda, N. Nemoto, K. Konishi, H. Takahashi, M. Kuwata-Gonokami, K. Matsumoto, and I. Shimoyama, "Enantiomeric switching of chiral metamaterial for terahertz polarization modulation employing vertically deformable MEMS spirals." *Nat. Commun.* vol. 6, pp. 8422 (2015).
- [25] H. S. Ee, and R. Agarwal, "Tunable metasurface and flat optical zoom lens on a stretchable substrate." *Nano Lett.* vol. 16, pp. 2818–2823 (2016).
- [26] W. Zhu, Q. Song, L. Yan, W. Zhang, P.-C. Wu, L. K. Chin, H. Cai, D. P. Tsai, Z. X. Shen, T. W. Deng, S. K. Ting, Y. Gu, G. Q. Lo, D. L. Kwong, Z. C. Yang, R. Huang, A. Q. Liu, and N. Zheludev. "A flat lens with tunable phase gradient by using random access reconfigurable metamaterial." *Adv. Mater.* vol. 27, pp. 4739–4743 (2015).
- [27] A. She, S. Zhang, S. Shian, D. R. Clarke, and F. Capasso, "Adaptive metalenses with simultaneous electrical control of focal length, astigmatism, and shift." *Sci. Adv.* vol.4, pp. eaap9957 (2018).
- [28] L. Cong, P. Pitchappa, C. Lee, and R. Singh, "Active phase transition via loss engineering in a terahertz MEMS metamaterial." *Adv. Mater.* vol. 29, pp. 1700733 (2017).
- [29] L. Cong, P. Pitchappa, Y. Wu, L. Ke, C. Lee, N. Singh, H. Yang, and R. Singh, "Active multifunctional microelectromechanical system metadevices: Applications in polarization control, wavefront deflection, and holograms." *Adv. Opt. Mater.* vol. 5, pp. 1600716 (2016).
- [30] J. Y. Ou, E. Plum, J. Zhang, and N. I. Zheludev, "An electromechanically reconfigurable plasmonic metamaterial operating in the near-infrared." *Nat. Nanotechnol.* vol. 8, pp. 252–255 (2013).
- [31] X. Zhao, K. Fan, J. Zhang, G. R. Keiser, G. Duan, R. D. Averitt, and X. Zhang. "Voltage-tunable dual-layer terahertz metamaterials." *Microsyst. Nanoeng.* vol. 2, pp. 16025 (2016).
- [32] C. M. Watts, X. Liu, and W. J. Padilla, "Metamaterial electromagnetic wave absorbers." *Adv. Mater.* vol. 24, pp. OP98–OP120 (2012).
- [33] A. Tittl, A. Leitits, M. Liu, F. Yesilkoy, D.-Y. Choi, D. N. Neshev, Y. S. Kivshar, and H. Altug, "Imaging-based molecular barcoding with pixelated dielectric metasurfaces." *Science* vol. 360, pp. 1105–1109 (2018).
- [34] C. Belacel, Y. Todorov, S. Barbieri, D. Gacemi, I. Favero, and C. Sirtori, "Optomechanical terahertz detection with single meta-atom resonator." *Nat. Commun.* vol. 8, pp.1578 (2017).
- [35] H. Tao, E. A. Kadlec, A. C. Strikwerda, K. Fan, W. J. Padilla, R. D. Averitt, E. A. Shaner, and X. Zhang. "Microwave and terahertz wave sensing with metamaterials." *Opt. Express* vol. 19, pp. 21620–21626 (2011).
- [36] F. Alves, D. Grbovic, B. Kearney, and G. Karunasiri, "Microelectromechanical systems bimaterial terahertz sensor with integrated metamaterial absorber." *Opt. Lett.* vol. 37, pp. 1886 (2012).
- [37] Z. Qian, S. Kang, V. Rajaram, C. Cassella, N. E. McGruer, and M. Rinaldi. "Zero-power infrared digitizers based on plasmonically enhanced micromechanical photoswitches." *Nat. Nanotechnol.* vol. 12, pp. 969 (2017).
- [38] X. Zhao, C. Chen, A. Li, G. Duan, and X. Zhang, "Implementing infrared metamaterial perfect absorbers using dispersive dielectric spacers." *Opt. Express* vol. 27, pp. 1727–1739, (2019).
- [39] X. Zhao, G. Duan, K. Wu, S.W. Anderson, and X. Zhang, "Intelligent metamaterials based on nonlinearity for magnetic resonance imaging." *Adv. Mater.* vol. 31, pp. 1905461 (2019)
- [40] X. Zhao, K. Wu, C. Chen, T. G. Bifano, S. W. Anderson, and X. Zhang, "Nonreciprocal magnetic coupling using nonlinear meta-atoms." *Adv. Sci.* vol. 7, pp. 2001443 (2020).